6382 *Chem. Mater.* **2007,** *19,* 6382–6384

High Mobility Organic Field-Effect Transistor Based on Hexamethylenetetrathiafulvalene with Organic Metal Electrodes

Yukihiro Takahashi,[†,*] Tatsuo Hasegawa,[†,*]
Sachio Horiuchi,[†] Reiji Kumai,[†] Yoshinori Tokura,[†,‡] and
Gunji Saito[§]

Correlated Electron Research Center (CERC), National Advanced Institute of Industrial Science and Technology (AIST), Tsukuba 305-8562, Department of Applied Physics, The University of Tokyo, Tokyo 113-8656, and Division of Chemistry, Kyoto University, Kyoto, 606-8502, Japan

Received September 19, 2007

In recent years, a large number of molecular materials with relatively high carrier mobilities have been reported for the use as channels of organic field-effect transistors (OFETs), which are envisioned as key components of low-cost, large-area, and flexible electronic devices.[1–7] Attention is being focused on modifications of polycyclic aromatic hydrocarbons like pentacene to realize a high performance and easy processability.[2–4] Other potential candidates are tetrathiafulvalene (TTF) analogues, which are well-known as electron-donor molecules in organic charge-transfer (CT) complexes.[8] The ability of these compounds to form a wide variety of organic metals and superconductors should permit their use in high-performance, single-component semiconducting materials. In fact, a mobility of about 0.1–1.4 cm^2/Vs has been reported for some TTF analogues.[6,7] In addition, the higher solubility of these molecules, compared with polyacenes, is advantageous as it permits low-cost solution processing.

In this communication, we report that the OFETs based on solution-grown as well as vapor-transport grown hexamethylenetetrathiafulvalene **1** (HMTTF; $C_{12}H_{12}S_4$)[9] single crystals exhibit a field-effect mobility exceeding 7–10 cm^2/Vs. To achieve this high device performance we found it necessary to optimize carrier injections at the source/drain contacts by using TTF-TCNQ thin-film electrodes (TCNQ = tetracyanoquinodimethane).[10]

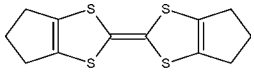

1

Yellow-colored and elongated-block single crystals of HMTTF with a typical size of $0.8 \times 0.2 \times 0.2$ mm^3 were obtained both by vapor transport with N_2 gas and by recrystallization from chlorobenzene solution in darkness. In the former process, care was taken to halt the crystal growth after about 2 days, because the color of the crystal surface turned into dark brown possibly as a result of thermal degradation of the molecules in longer runs of crystal growth. In the latter process, on the other hand, crystals were obtained over a longer term of several weeks at room temperature. The solution- as well as vapor-transport grown products formed the identical monoclinic crystal structure with space group $P2_1/c$ and unit cell parameters of $a = 6.376(6)$ Å, $b = 14.54(1)$ Å, $c = 12.92(1)$ Å, and $\beta = 94.689(16)°$ ($Z = 4$). The packing motif is shown in Figure 1. An intermolecular *side-by-side* arrangement along the *a*-axis affords large π–π interactions with close S–S contacts of 3.545(3)–3.647(3) Å. On the other hand, molecules are stacked along the *b*-axis in a *brickwork* arrangement in which molecules are slipped by half their length along the molecular long axes. For crystallographically independent three intermolecular contacts shown in Figure 1, the transfer integrals were estimated by extended Hückel molecular orbital calculations;[8] $t_1 = 0.1151$ eV (*side-by-side*), $t_2 = -0.0113$ eV (*slipped stack*), and $t_3 = 0.0176$ eV (*slipped stack*).

Single-crystal OFETs with parylene C gate dielectric layers were fabricated as reported previously.[10] The dielectric thickness we used is 1.0 μm with gate capacitance of about 1.90–2.12 nF/cm^2. We used thermally evaporated Au, Ag, or TTF-TCNQ metallic thin films as the source/drain electrodes. The sheet resistance of the TTF-TCNQ films is 1–1.5 kΩ at the thickness of about 300 nm. Typical channel length L and width W is about 100 μm. All the properties of the transistors were measured with a source/drain current along the *a*-axes which correspond to the direction of the longest dimension of the crystal.

Transfer characteristics of the devices are shown altogether in Figure 2 in linear scale. All the devices exhibited p-type feature, the size of which depended significantly on the kinds of electrodes. The mobility of the device was calculated by using the standard formula in the linear region; $\mu_{\text{lin}} = (dI_D/dV_G)[L/(WC_iV_D)]$, where I_D, V_D, V_G, and C_i are drain current,

---

[†] Advanced Institute of Industrial Science and Technology (AIST).
[‡] The University of Tokyo.
[§] Kyoto University.

(1) Würthner, F.; Schmidt, R. *ChemPhysChem* **2006**, *7*, 793–797.
(2) Menard, E.; Podzorov, V.; Hur, S.-H.; Gaur, A.; Gershenson, M. E.; Rogers, J. A. *Adv. Mater.* **2004**, *16*, 2097–2101.
(3) Payne, M. M.; Parkin, S. R.; Anthony, J. E.; Kuo, C.-C.; Jackson, T. N. *J. Am. Chem. Soc.* **2005**, *127*, 4986–4987.
(4) Schmidt, R.; Gottling, S.; Leusser, D.; Stalke, D.; Krause, A.; Würthner, F. *J. Mater. Chem.* **2006**, *16*, 3708–3714.
(5) Yamamoto, T.; Takimiya, K. *J. Am. Chem. Soc.* **2007**, *129*, 2224–2225.
(6) (a) Mas-Torrent, M.; Durkut, M.; Hadley, P.; Ribas, X.; Rovira, C. *J. Am. Chem. Soc.* **2004**, *126*, 984–985. (b) Mas-Torrent, M.; Rovira, C *J. Mater. Chem.* **2006**, *16*, 433–466.
(7) (a) Naraso; Nishida, J.; Ando, S.; Yamaguchi, J.; Itaka, K.; Koinuma, H.; Tada, H.; Tokito, S.; Yamashita, Y. *J. Am. Chem. Soc.* **2005**, *127*, 10142–10143. (b) Naraso Nishida, J.; Kumaki, D.; Tokito, S.; Yamashita, Y. *J. Am. Chem. Soc.* **2006**, *128*, 9598–9599.
(8) (a) Mori, T.; Kobayashi, A.; Sasaki, Y.; Kobayashi, H.; Saito, G. *Bull. Chem. Soc. Jpn.* **1984**, *57*, 627. (a) Ishiguro, T.; Yamaji, K.; Saito, G. *Organic Superconductors*; 2nd ed.; Springer Verlag: Berlin, 1998.
(9) Greene, R. L.; Mayerle, R.; Schumaker, R.; Castro, C.; Chaikint, P. M.; Etemad, S.; Laplaca, S. J. *Solid State Commun.* **1976**, *20*, 943–946.
(10) (a) Takahashi, Y.; Hasegawa, T.; Abe, T.; Tokura, Y.; Nishimura, K.; Saito, G. *Appl. Phys. Lett.* **2005**, *86*, 063504-1–063504-3. (b) Takahashi, Y.; Hasegawa, T.; Abe, Y.; Tokura, Y.; Saito, G. *Appl. Phys. Lett.* **2006**, *88*, 073504-1–073504-3. (c) Hiraoka, M.; Hasegawa, T.; Abe, Y.; Yamada, T.; Tokura, Y.; Yamochi, H.; Saito, G.; Akutagawa, T.; Nakamura, T. *Appl. Phys. Lett.* **2006**, *89*, 173504-1–173504-3.

10.1021/cm702690w CCC: $37.00

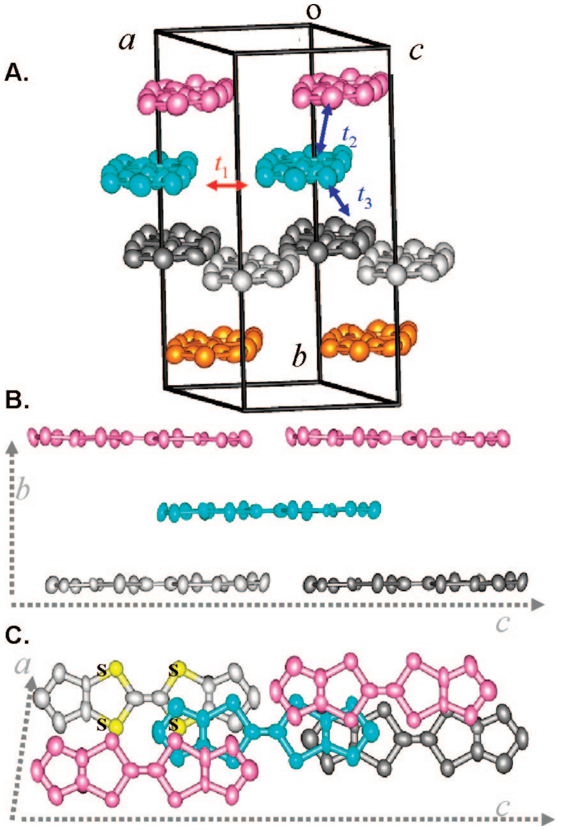

Figure 1. [A] Crystal structure of HMTTF single crystals grown both by vapor transport and by recrystallization. The *brickwork* packing motif is shown with the view parallel [B] and perpendicular [C] to the molecular planes.

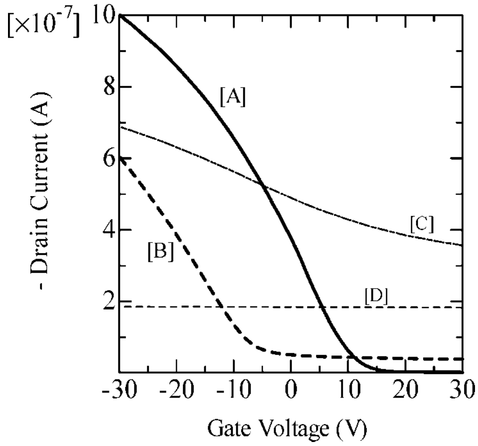

Figure 2. Transfer characteristics of HMTTF single crystal transistor with a variety of source/drain electrodes; [A and B] with TTF-TCNQ electrodes (V_D = –1 V), [C] with Ag electrodes (V_D = –5 V), and [D] with Au electrodes (V_D = –1 V).

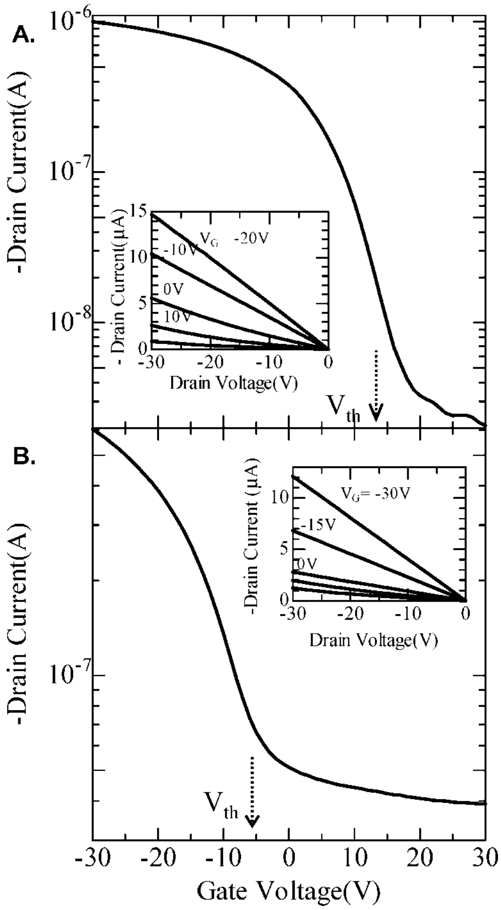

Figure 3. Transfer and output (inset) characteristics of OFETs composed of single crystals grown by [A] vapor transport and [B] recrystallization.

drain voltage, gate voltage, and gate dielectric capacitance per unit area. We note that there is no serious leakage path outside the channel, because the *W* is limited by the size of the single crystals. The result for the device with TTF-TCNQ thin-film electrodes was estimated as about 2–10 cm^2/Vs (average value was 7 cm^2/Vs among 12 devices examined) in the linear region, while devices with Ag or Au electrodes showed much lower mobilities of about 0.12 cm^2/Vs and 0.02 cm^2/Vs, respectively, with larger off currents. It is clear from this that the use of TTF-TCNQ organic metal electrodes is essential to achieve a high performance with HMTTF OFETs. We consider that this higher performance is associated with several features of organic metal electrodes. First, the Fermi energy in TTF-TCNQ well matches with the valence band of HMTTF crystals, as the ionization potential of HMTTF (6.4 eV) is close to that of TTF (6.7 eV). This should lead to efficient hole injection into the channel semiconductors at the source/drain contacts. Second, compared with Au or Ag with high melting temperature (1064 °C for Au and 961 °C for Ag), TTF-TCNQ thin-film electrodes are fabricated by thermal evaporation at much lower temperatures (source temperature of only about 180 °C), which could suppress thermal damage to the crystal surfaces on which the electrodes are deposited during fabrication of the electrodes. These effects are useful to minimize the contact resistance at the source/drain electrodes, which should lead to the observation of real bulk mobility without voltage drops at the contacts.

Figures 3 shows the transfer characteristics of the best performance devices composed of (A) solution- and (B) vapor-transport grown channel single crystals, respectively, in logarithmic scale. In the devices, the field effect mobility in the linear region reached 11.2 cm^2/(Vs) in vapor-transport grown crystals and 10.4 cm^2/(Vs) in solution-grown ones. We note that the output characteristics shown in the inset present the sign of current saturation at high V_D range, if we presume the additional bulk current in the current–voltage characteristics.We found that the devices keep high performance at atmospheric conditions for several weeks. (The mobility of the former device was estimated as 7 cm^2/Vs after 2 months of fabrication). The high performance may be attributed to the close *side-by-side* and *brickwork* molecular packing of HMTTF, which is in contrast to the *herringbone* molecular arrangement of rather high mobility materials such as pentacene. We note that the above value is, to the best of our knowledge, second best for single-crystal OFETs[11] and the highest with solution-grown channel material. The results clearly demonstrate the high potential of the TTF analogues. The direct use of the single-crystal devices is also expected by possible low-cost solution patterning processes.[12]

As presented in Figure 3, a normally on state with threshold gate voltage (V_{th}) of 13 V and a high on/off ratio ($\sim$600) is observed in the device containing vapor-transported crystals, whereas a normally off state with V_{th} of about -6 V and a much lower on/off ratio (<3) is seen in the device containing solution-processed crystals. We note that similar difference in the V_{th} and on/off ratio is observed for all the devices with the vapor-transported and solution-processed crystals. Noticeable nonlinearity, or gate voltage-dependent mobility, is also seen in the former device. These different features give a clue to understanding the relationship between crystallinity and charge-carrier dynamics in the channel molecular semiconductors. We hypothesize that the vapor-transport grown crystals could include a larger number of bulk carriers inside the crystals, possibly associated with the thermal decomposition during the crystal growth at relatively high temperature. Bulk carriers could be depleted by the reverse gate biases. This may provide the origin of the normally on behavior in the transfer characteristics and low off current at high positive voltages, as observed in Figure 3A. In contrast, we also consider that the larger off-current, as observed in Figure 3B, is possibly associated with conductive paths remaining on the crystal surfaces during the drying process just after the recrystallization from solution. For example, adsorption of a tiny amount of CT compound (composed of HMTTF with some impurities) on the crystal surfaces could be the origin of large off current in the single crystal FET.[13] It may afford the conductive surface layer whose current is hardly eliminated by the reverse gate biases.

In summary, we identified a rather high mobility, exceeding 10 cm^2/Vs, in HMTTF OFETs composed of solution- as well as vapor-transport grown single crystals with TTF-TCNQ thin-film electrodes. This observed high performance can be attributed to the large π–π intermolecular interactions in HMTTF as well as to efficient carrier injections at the source/drain contacts achieved through the use of organic metal electrodes. The results indicate the potential of TTF analogues as channel semiconducting materials suitable for the fabrication of high-performance and low-cost devices.

Supporting Information Available: Experimental procedures (PDF) and X-ray crystallography files (CIF). This material is available free of charge via the Internet at http://pubs.acs.org.

CM702690W

---

(11) (a) Menard, E.; Podzorov, V.; Fur, S.-H.; Gaur, A.; Gershenson, M. E.; Rogers, J. A. *Adv. Mater.* **2004**, *16*, 2097–2101. (b) Takeya, J.; Yamagishi, M.; Tominari, Y,; Hirahara, R.; Nakazawa, Y.; Nishikawa, T.; Kawase, T,; Shimoda, T.; Ogawa, S. *Appl. Phys. Lett.* **2007**, *90*, 102120-1–102120-3.

(12) Briseno, A. L.; Mannsfeld, S. C. B.; Ling, M. M.; Liu, S.; Tseng, R. J.; Reese, C.; Roberts, M. E.; Yang, Y.; Wudl, F.; Bao, Z. *Nature (London)* **2006**, *444*, 913–917.

(13) Qui, Y.; Hu, Y. C.; Dong, G. F.; Wang, L. D.; Xie, J. F.; Ma, Y. N. *Appl. Phys. Lett.* **2003**, *83*, 1644–1646.